Electronic Supplementary Material (ESI) for Journal of Materials Chemistry A.

Experimental

Materials

Sodium hypophosphite monohydrate ($NaH_2PO_2·H_2O$), metal precursors including cobalt chloride hexahydrate ($CoCl_2·6H_2O$), cobalt nitrate hexahydrate [$Co(NO_3)_2·6H_2O$], cobalt acetate tetrahydrate [$Co(CH_3COO)_2·4H_2O$], iron nitrate nonahydrate [$Fe(NO_3)_3·9H_2O$)] and nickel nitrate hexahydrate [$Ni(NO_3)_2·6H_2O$] were purchased from Sigma-Aldrich Corporation. All chemicals were used as received without purification. Metal substrates, such as nickel foams (NF) and copper foils, were purchased from standard sources. Prior to use, these substrates were cut into pieces (1 cm × 1.5 cm), rinsed successively with acetone, ethanol and deionized water by ultrasonication to remove the impurities, and finally blown-dry with nitrogen gas.

Electrodeposition of Co_2P on NF

0.01 M of metal precursor and 0.1 M of $NaH_2PO_2·H_2O$ were mixed in 20 mL of deionized water and magnetically stirred for 15 min to form a clear precursor solution. Electrodeposition of cobalt phosphides was performed on a CHI 660D electrochemical workstation under room temperature. A three-electrode configuration was used, in which the washed NF was directly used as the working electrode (the geometric area exposed to the solution was ~1.0 cm^{-2}), a platinum (Pt) foil as the counter electrode and a saturated calomel electrode (SCE) as the reference electrode. A potential of -1.0 V vs. SCE was applied for the electrodeposition for 10 min. Subsequently, the as-deposited NF was taken out from the solution, rinsed thoroughly with deionized water and then blown-dry with nitrogen gas for further use. Cobalt phosphides electrodeposited from cobalt chloride hexahydrate, cobalt acetate tetrahydrate and cobalt nitrate hexahydrate were named as Co_2P(C), Co_2P(A) and Co_2P(N), respectively, after the initials of the anions of cobalt precursors. Other Co_2P structures were synthesized for comparison by the same synthetic conditions, except that the concentration of $CoCl_2·6H_2O$ was increased to 0.05, 0.1 and 0.2 M.

Characterizations

Scanning electron microscopy (SEM) images were taken on a JEOL JSM-7001F field-emission scanning electron microscope. High-resolution transmission electron microscopy (HRTEM) images were acquired on a Philips CM300 transmission electron microscope. X-ray diffraction (XRD) spectrum was achieved on a Philips X-ray diffractometer with Cu Kα radiation (λ = 1.541Å), in which the samples electrodeposited on a copper foil was used due to its flat surface. X-ray photoelectron spectroscopy (XPS) spectra were obtained on a VG Thermo Escalab 220i-XL X-ray photoelectron spectroscopy system. Element analysis was performed on an Oxford Instruments energy dispersive X-

ray (EDX) spectroscopy. Ultraviolet-visible (UV-vis) absorption spectra were attained on a Shimadzu UV-3600 UV-vis spectrophotometer, in which the Co_2P(C)/NF and bare NF were directly used. Solar intensity was measured by a Daystar DS-05 solar meter under the real sun. Thermal images were taken by an FLIR E50 thermal imaging infrared camera.

Electrochemical measurements

All the electrochemical measurements of the cobalt phosphides were recorded on a CHI 660D electrochemical work station, with 1 M KOH aqueous solution as the electrolyte. A three-electrode configuration was used, with Co_2P/NF directly as the working electrode, a Pt foil as the counter electrode and an SCE as the reference electrode. Linear sweep voltammetry (LSV) curves were performed at a scan rate of 5 mV s^{-1}. Cyclic voltammetry (CV) curves were measured at different scan rates of 10, 20, 50, 100 and 200 mV s^{-1}. Electrochemical impedance spectra (EIS) were achieved in the frequency range of 0.01 to 100 kHz with 5 mV amplitude. Current density versus time (*i*-*t*) curves of Co_2P(C) were carried out in 1 M KOH solution at their respective overpotentials. The measurements under the real sun were carried out from 10:00 to 11:00 am on 27th October 2016 (the ambient temperature is 32 °C). The as-measured potentials were converted to reversible hydrogen electrode (RHE) based on the following equation:

$$E_{RHE}\ (V) = E_{SCE}\ (V) + E^0_{SCE} + 0.059 \times pH$$

E^0_{SCE} is actually temperature-dependent, as shown in Table S1 below:

Table S1 E^0_{SCE} at different temperatures

T (°C)	E^0_{SCE}
25	0.241
35	0.234
45	0.227
55	0.220
65	0.212

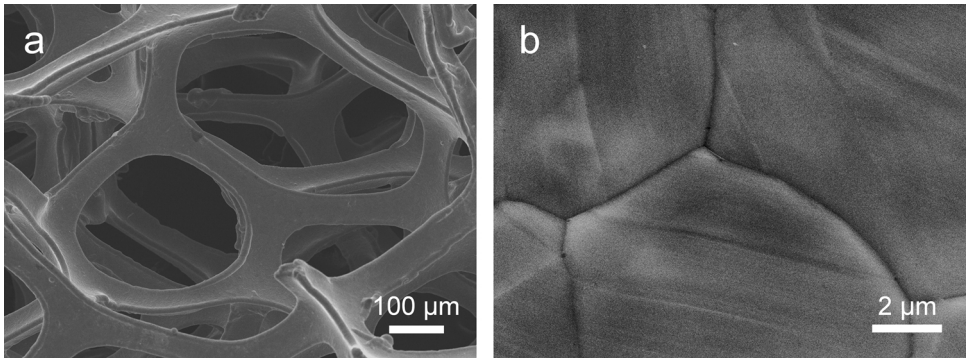

Fig. S1 (a) Low- and (b) high-magnification SEM images of bare NF.

Bare nickel foam (NF) presents a macro-porous framework with smooth surface.

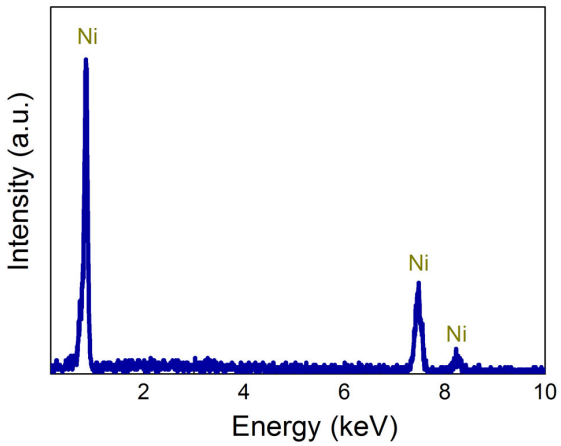

Fig. S2 EDX spectrum of bare NF.

EDX spectrum indicates that bare NF contains Ni element only.

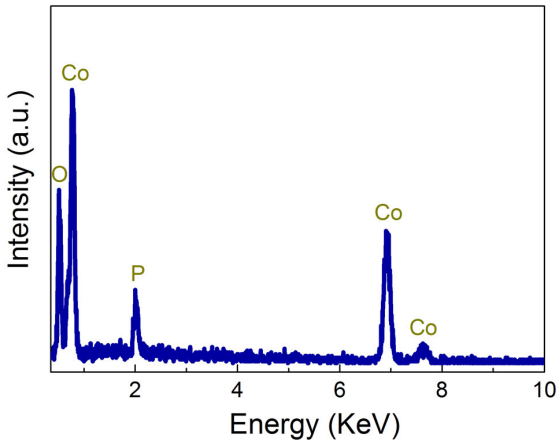

Fig. S3 EDX spectrum of Co_2P(C) powder removed from the underlying substrate.

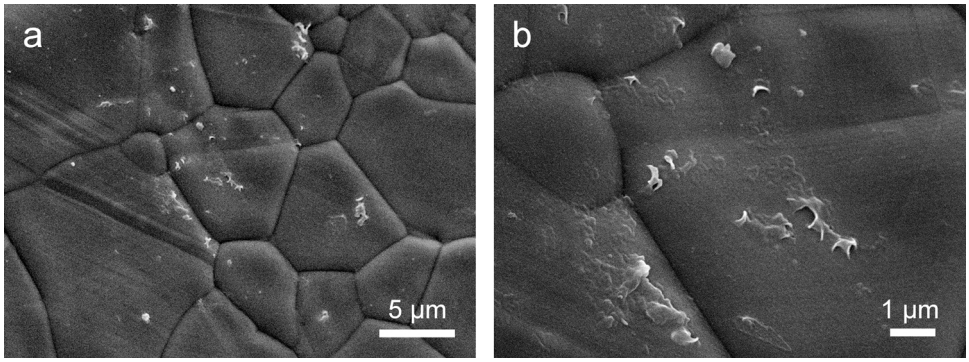

Fig. S4 (a) Low- and (b) high-magnification SEM images of NF immersed in the same electrodeposition precursor solution for 10 min without applied potentials.

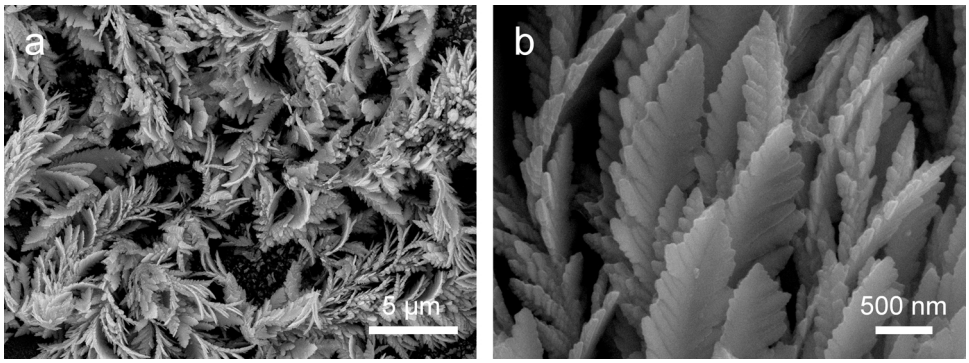

Fig. S5 (a) Low- and (b) high-magnification SEM images of Co_2P(A).

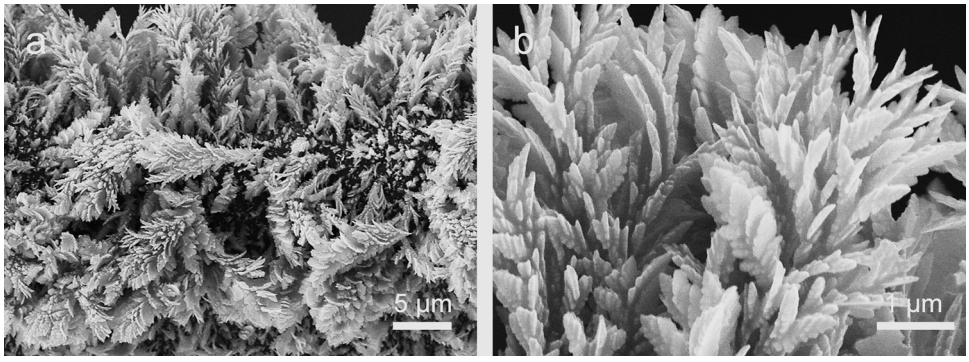

Fig. S6 (a) Low- and (b) high-magnification SEM images of Co_2P(N).

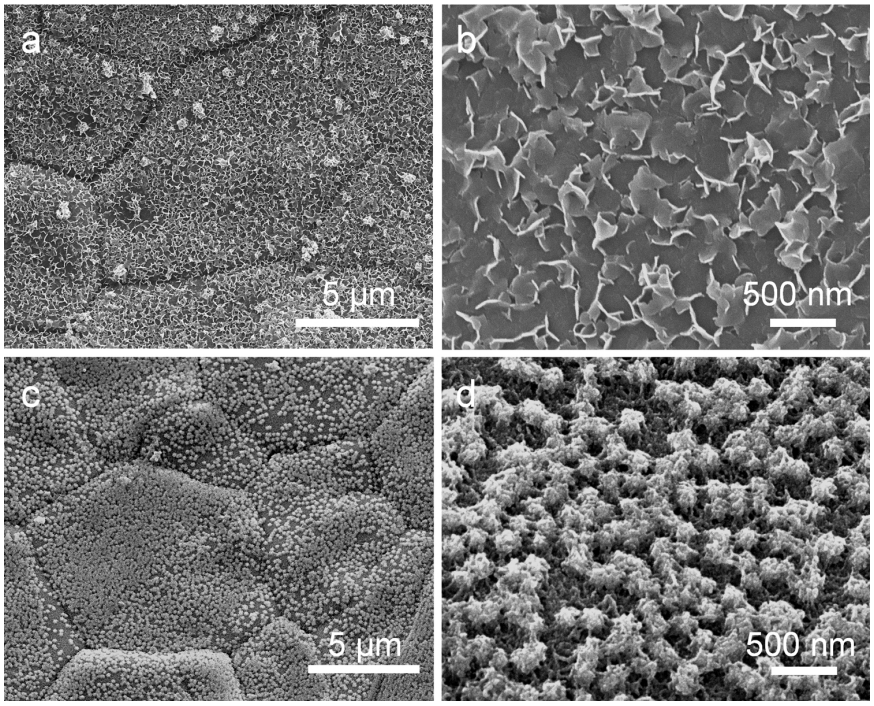

Fig. S7 Low- and high-magnification SEM images of (a,b) iron phosphide nanosheets and (c,d) nickel phosphide nanoclusters.

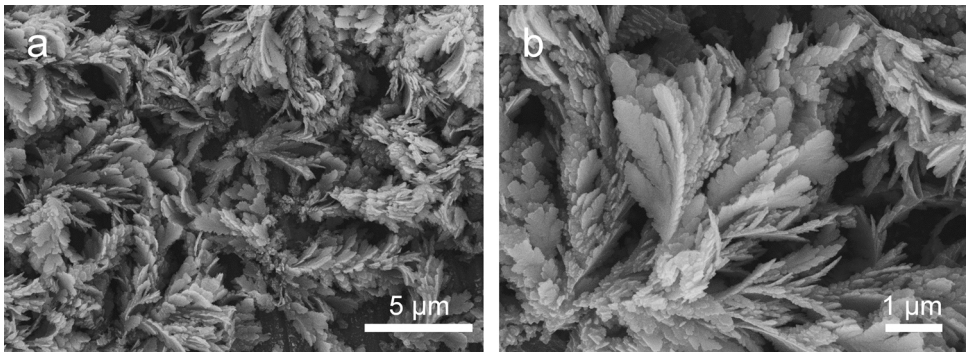

Fig. S8 (a) Low- and (b) high-magnification SEM images of Co_2P(N) electrodeposited on a copper foil.

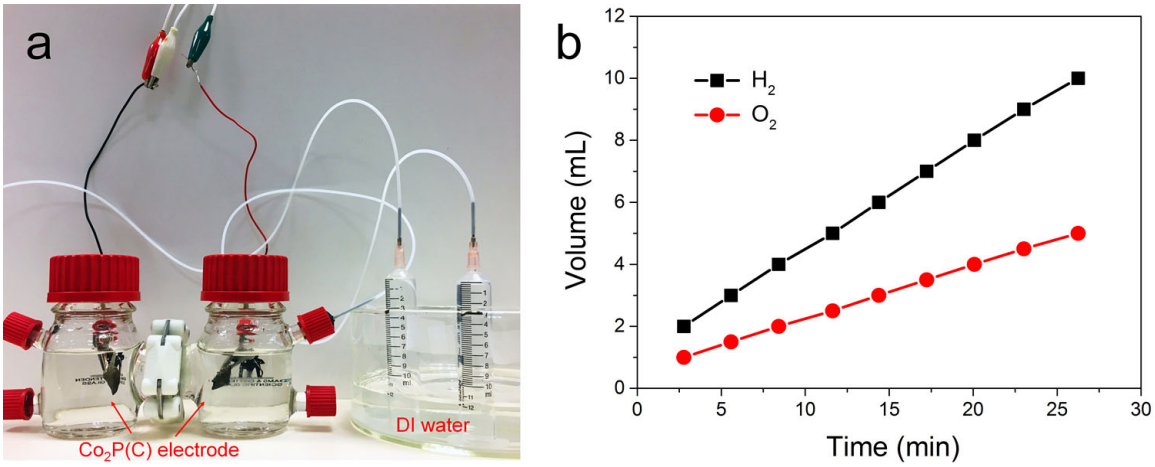

Fig. S9 (a) Digital photos of the overall water splitting setup with Co_2P(C) as both cathode and anode (1 M KOH electrolyte). (b) The volume of the generated gases with reaction time.

The overall water splitting setup comprises of two quartz bottles that are well connected by a thin Nafion membrane, each containing a Co_2P(C) electrode, one as cathode and the other as anode. Two sealed syringes connecting to the cathode and anode bottle, respectively, were used to collect the generated gas.

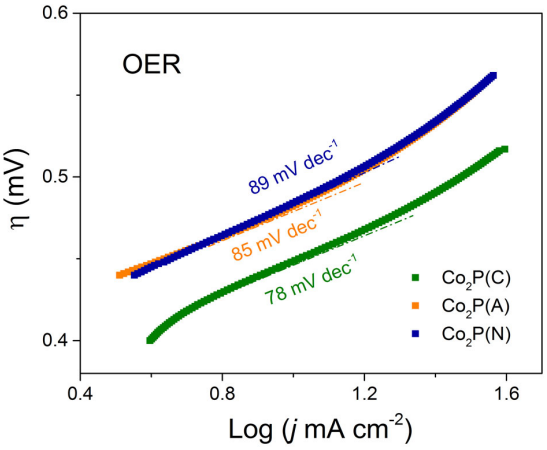

Fig. S10 OER Tafel plots of different Co_2P measured in 1 M KOH electrolyte under room temperature.

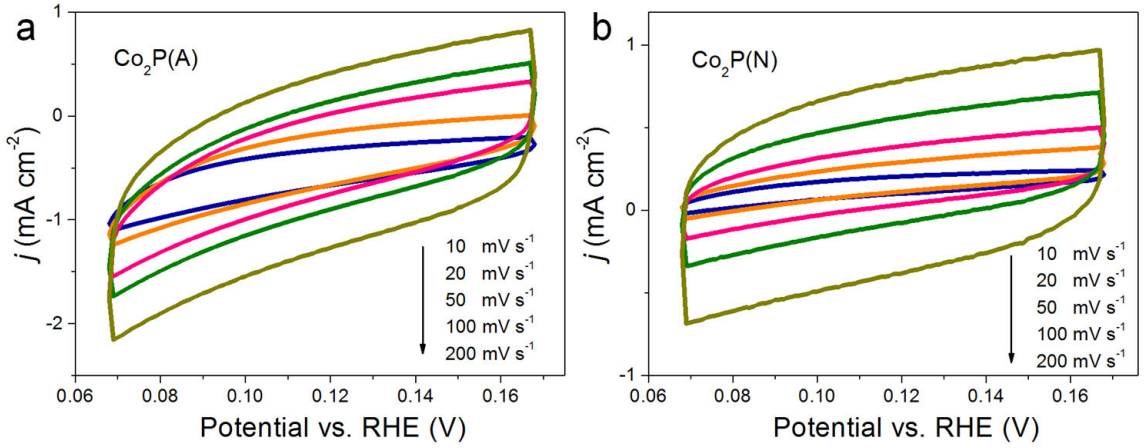

Fig. S11 CV curves of (a) Co_2P(A) and (b) Co_2P(N) at various scan rates of 10, 20, 50, 100 and 200 mV s^{-1}.

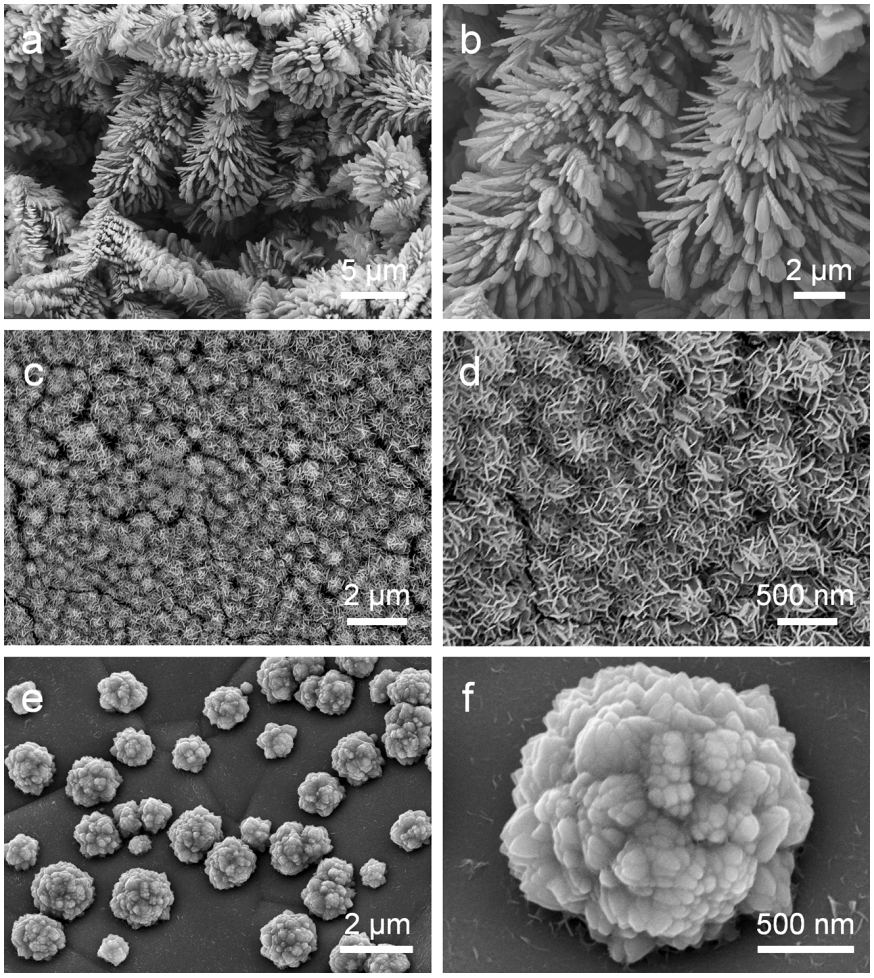

Fig. S12 Low- and high-magnification SEM images of Co_2P obtained at different $CoCl_2 \cdot 6H_2O$ concentrations of (a,b) 0.05 M, (c,d) 0.1 M and (e,f) 0.2 M.

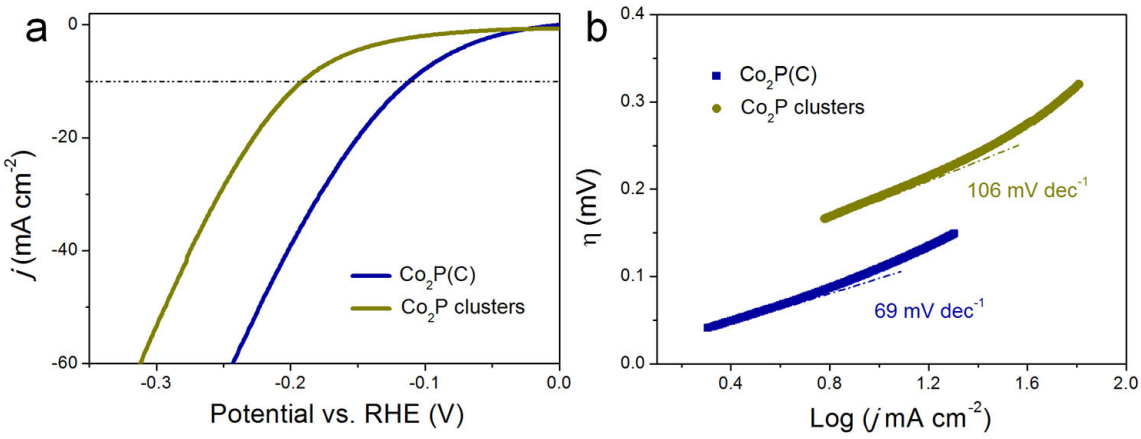

Fig. S13 (a) HER LSV curves and (b) Tafel plots of Co_2P(C) and Co_2P clusters (1 M KOH, room temperature).

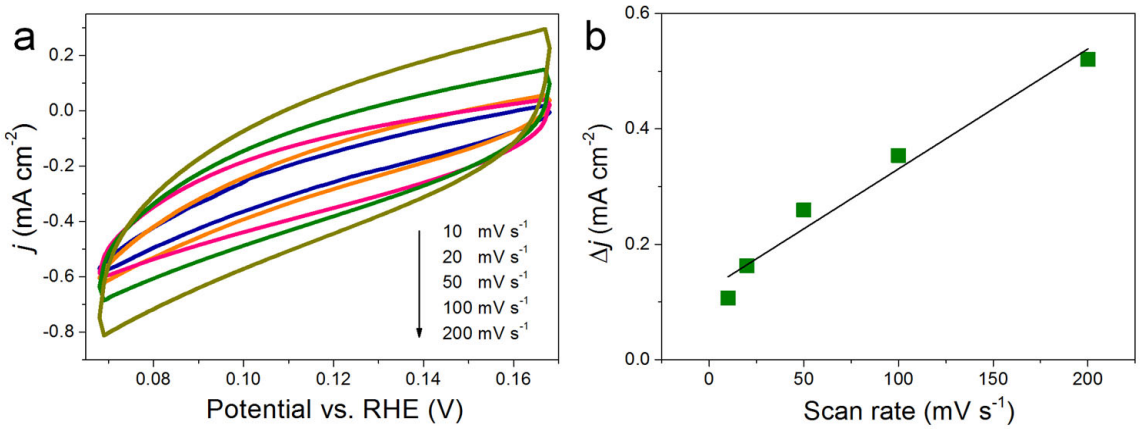

Fig. S14 (a) CV curves of Co_2P clusters at various scan rates of 10, 20, 50, 100 and 200 mV s^{-1}. (b) Charging current density differences of Co_2P clusters plotted against the scan rates.

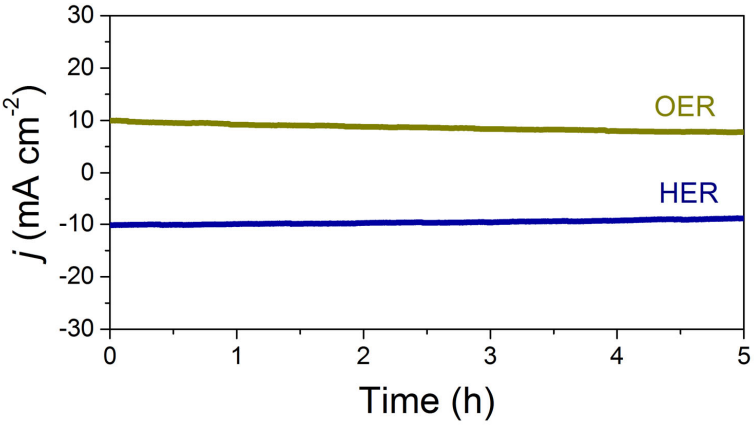

Fig. S15 Time-dependent current density curves of Co_2P(C) measured under a static overpotential of 108 mV for HER and 440 mV for OER (1 M KOH).

Co_2P(C) can maintain up to 95% (HER) and 86% (OER) of its current density at 10 mA cm^{-2} after 5 hours, demonstrating its good durability.

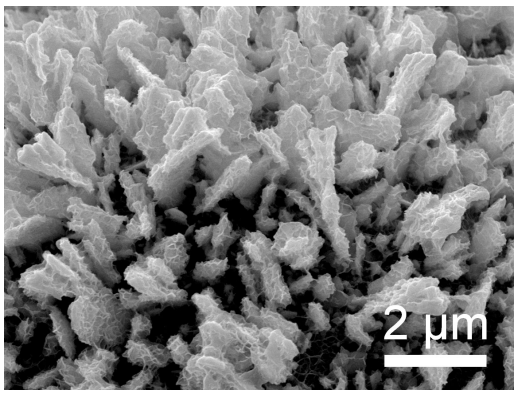

Fig. S16 SEM image of Co_2P(C) after long-term measurements.

The superstructures of Co_2P(C) are mostly retained after electrocatalytic measurements in 1 M KOH for 5 h.

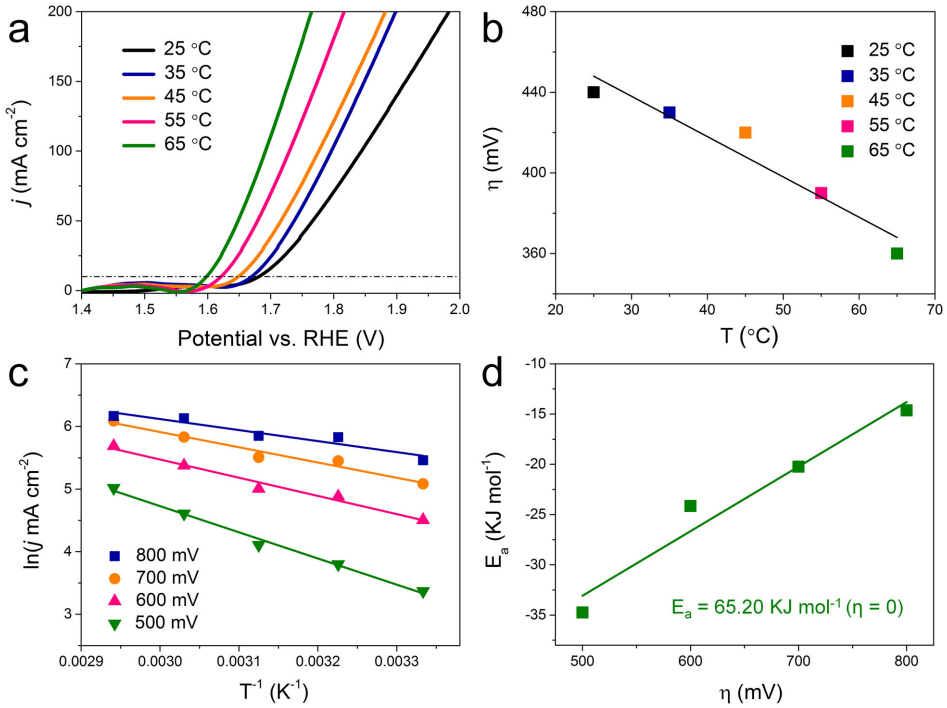

Fig. S17 (a) OER LSV curves of $Co_2P(C)$ measured under the real sun (1 M KOH electrolyte). (b) The decrease of overpotential (j = 10 mA cm^{-2}) with the increase of temperature. (c) Semilogarithmic dependence of current density versus temperature (Arrhenius plots) at overpotentials of 500, 600, 700 and 800 mV. (d) Linearly fitted activation energy curve of $Co_2P(C)$.

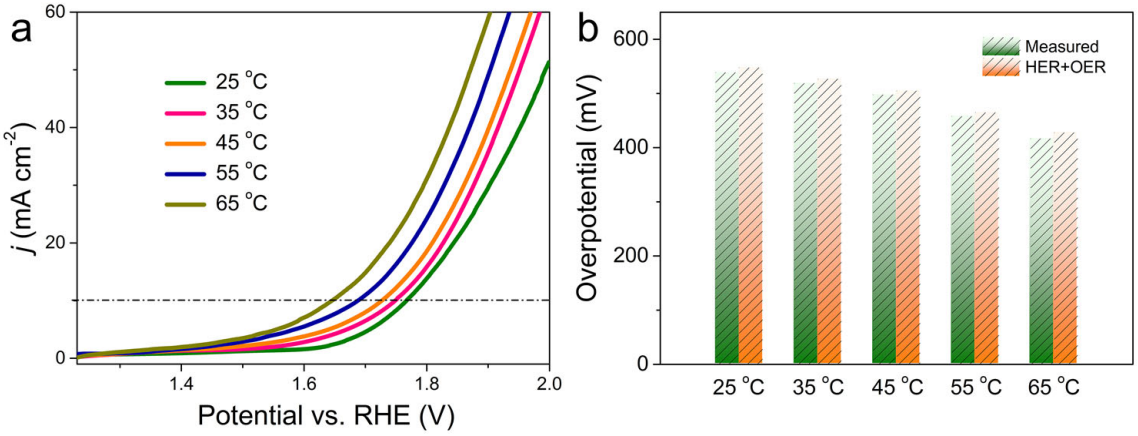

Fig. 18 (a) LSV curves of $Co_2P(C)$ overall water splitting under room temperature and increased temperatures heated from solar irradiation. (b) Comparison of the measured overpotentials of overall water splitting and separately measured HER and OER overpotentials.

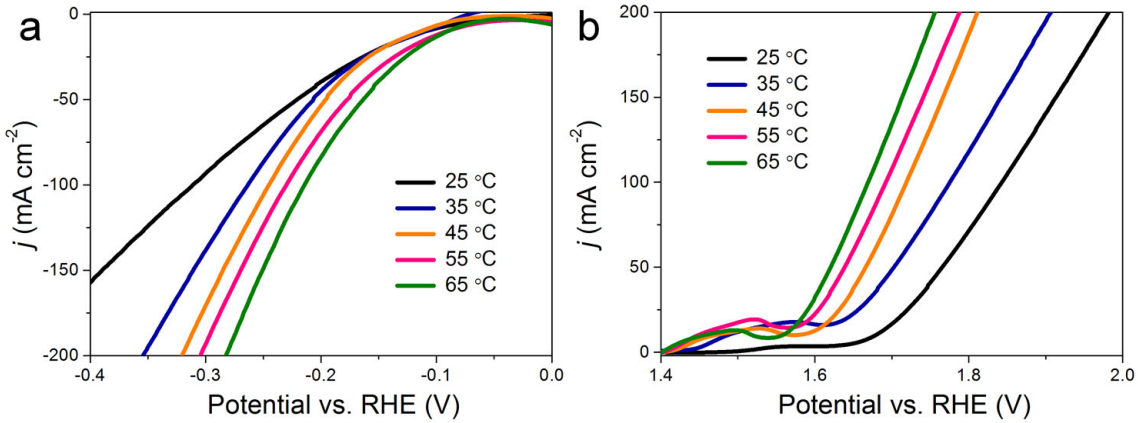

Fig. S19 (a) HER and (b) OER LSV curves of Co_2P(C) measured under different temperatures directly heated by water bath (1 M KOH).

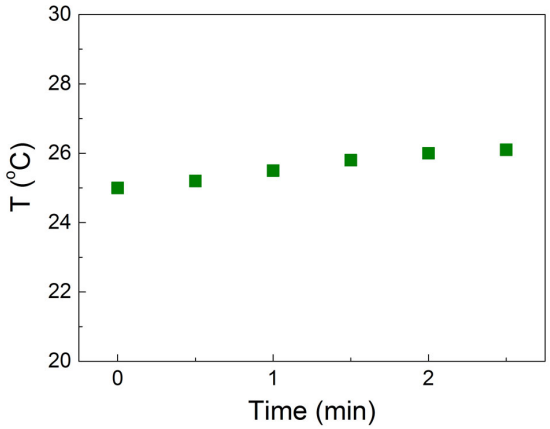

Fig. S20 The temperatures of KOH electrolyte illuminated by a full-spectrum LED lamp under room temperature.

The full-spectrum LED lamp causes a temperature increase of less than 1 °C, which can be considered negligible for the electrocatalysis.

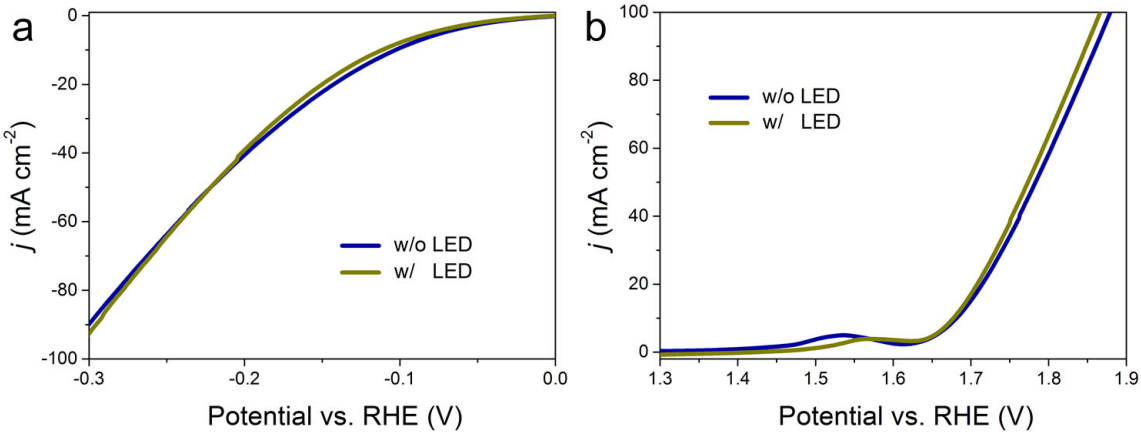

Fig. S21 (a) HER and (b) OER LSV curves of Co_2P(C) measured with and without the irradiation of a full-spectrum LED (room temperature).

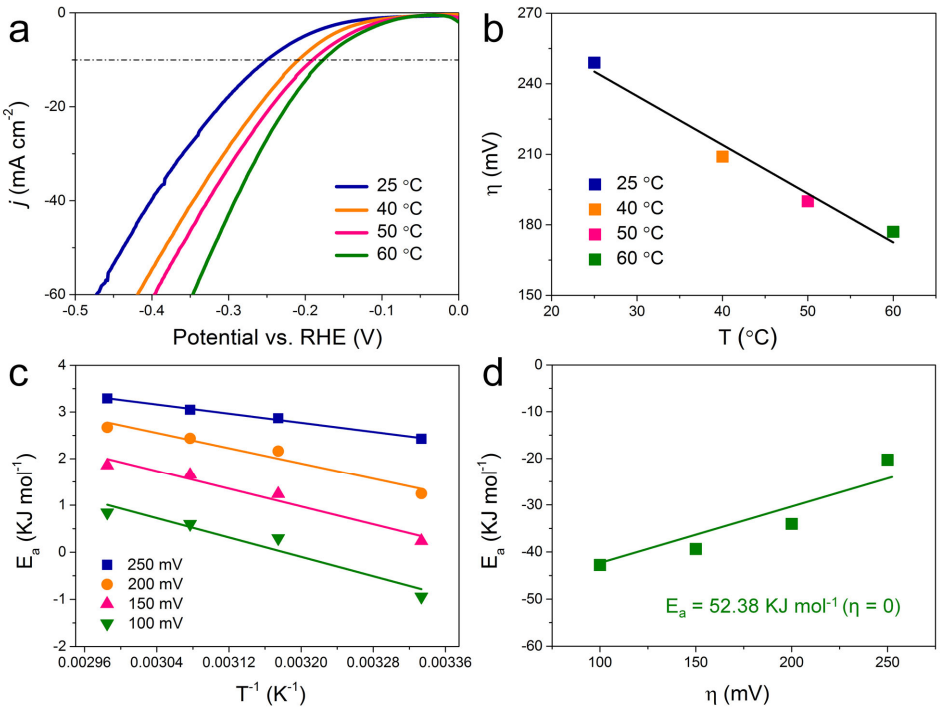

Fig. S22 (a) HER LSV curves of bare NF measured under natural sunlight (1 M KOH electrolyte). (b) The decrease of overpotential (j = 10 mA cm^{-2}) with the increase of temperature. (c) Semilogarithmic dependence of current density versus temperature (Arrhenius plots) at overpotentials of 100, 150, 200 and 250 mV. (d) Linearly fitted activation energy curve of bare NF.

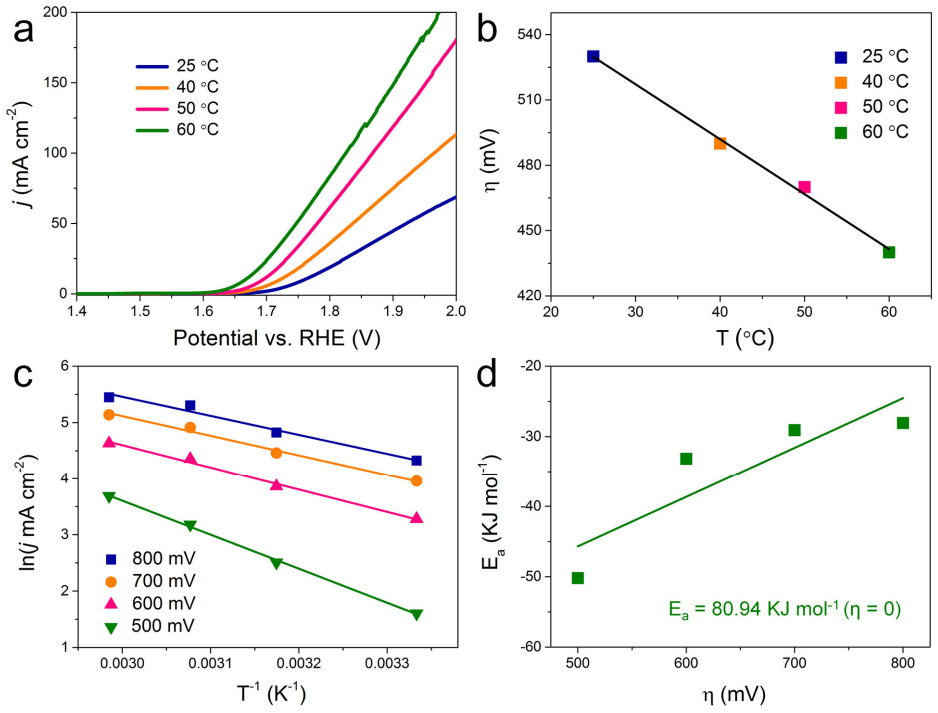

Fig. S23 (a) OER LSV curves of bare NF measured under natural sunlight (1 M KOH electrolyte). (b) The decrease of overpotential (j = 10 mA cm^{-2}) with the increase of temperature. (c) Semilogarithmic dependence of current density versus temperature (Arrhenius plots) at overpotentials of 500, 600, 700 and 800 mV. (d) Linearly fitted activation energy curve of bare NF.

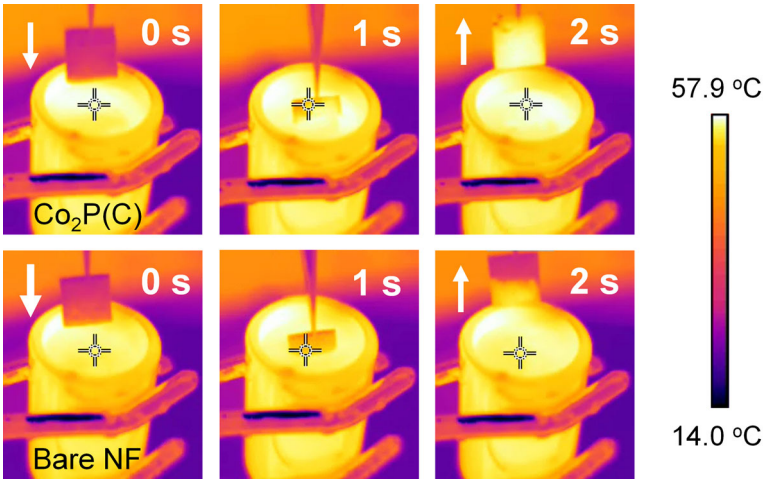

Fig. S24 Thermal images of (top) $Co_2P(C)$ and (bottom) bare NF taken out from hot KOH electrolyte.

Table S2 A comparison of the HER activity of Co_2P(C) superstructures with recently reported phosphide-based electrocatalysts measured in alkaline media

Catalyst	Substrate	Electrolyte	η (mV) at 10 mA cm^{-2}	Tafel slope (mV dec^{-1})	Reference
Cobalt phosphide films	Ni Ti Au	0.1 M KOH	411 577 312	147 121 100	*RSC Adv.*, 2015, **5**, 105814-105819
Ni_2P microsphere/Ni superstructures	Ni foam	1 M KOH	98	72	*ACS Catal.*, 2016, **6**, 714-721
Cobalt phosphide nanosheets/carbon	Glassy carbon electrode	1 M KOH	111	70.9	*Green Chem.*, 2016, **18**, 2287-2295
Ni-modified cobalt phosphide nanoparticles	Glassy carbon electrode	1 M KOH	180	63	*J. Mater. Chem. A*, 2016, **4**, 7549-7554
Co-P film	Cu foil	1 M KOH	94	42	*Angew. Chem. Int. Ed.*, 2015, **54**, 6251-6254
CoP nanoneedle arrays	Carbon cloth	1 M KOH	95	69	*ChemSusChem*, 2016, **9**, 472-477
Co_2P film	Co foil	1M KOH	183	N/A	*ACS Appl. Mater. Interfaces*, 2016, **8**, 12798-12803
NiFeP	NiFe foil	1M KOH	255	N/A	*ACS Appl. Mater. Interfaces*, 2016, **8**, 12798-12803
Ni_5P_4 film	Ni foil	1M KOH	150	53	*Angew. Chem. Int. Ed.*, 2015, **54**, 12361-12365
CoP nanoparticles	Ti foil	1M KOH	~170	N/A	*Nano Energy*, 2016, **29**, 37-45
Nickel phosphides	Carbon fibre paper	1 M KOH	160	107.3	*ACS Appl. Mater. Interfaces*, 2016, **8**, 10826-10834
Co_2P encapsulated in N,P-doped graphene	Glassy carbon electrode	1M KOH	~180	96	*Nano Lett.*, 2016, **16**, 4691-4698
FeP nanorod arrays	Carbon cloth	1M KOH	~220	146	*ACS Catal.*, 2014, **4**, 4065-4069
Cobalt phosphide nanowire arrays	Carbon cloth	1M KOH	209	129	*J. Am. Chem. Soc.*, 2014, **136**, 7587-7590

Table S3 A comparison of the OER activity of $Co_2P(C)$ superstructures with recently reported phosphide-based electrocatalysts measured in alkaline media

Catalyst	Substrate	Electrolyte	η (mV) at 10 mA cm^{-2}	Tafel slope (mV dec^{-1})	Reference
Cobalt phosphide/ cobalt nitride embedded nitrogen-rich nanocarbons	Glassy carbon electrode	0.1 M KOH	390	78	*J. Mater. Chem. A*, 2016, **4**, 10575-10584
CoP hollow polyhedron	Glass carbon electrode	1 M KOH	400	57	*ACS Appl. Mater. Interfaces*, 2016, **8**, 2158-2165
Co_2P film	Co foil	1 M KOH	367	N/A	*ACS Appl. Mater. Interfaces*, 2016, **8**, 12798-12803
Porous nickel phosphide nanoplates	Glass carbon electrode	1 M KOH	300	64	*Energy Environ. Sci.*, 2016, **9**, 1246-1250
Co-P film	Cu foil	1 M KOH	345	47	*Angew. Chem. Int. Ed.*, 2015, **54**, 6251-6254
CoP NPs	Glass carbon electrode	1 M KOH	342	90	*ChemElectroChem*, 2016, **3**, 719-725
CoP nanoneedle arrays	Carbon cloth	1 M KOH	281	N/A	*ChemSusChem*, 2016, **9**, 472-477
Co_2P nanoneedles	Glass carbon electrode	1 M KOH	310	50	*ACS Energy Lett.*, 2016, **1**, 169-174
Nickel phosphides	Carbon fibre paper	1 M KOH	320	72.2	*ACS Appl. Mater. Interfaces*, 2016, **8**, 10826-10834
$(Co_{1-x}Fe_x)_2P$ ribbons	Co-Fe-P ingot	1 M KOH	270	40	*Energy Environ. Sci.*, 2016, **9**, 2257-2261
CoP nanowires	Ti mesh	1 M KOH	310	87	*Nanotechnology*, 2016, **27**, 23LT01
Porous cobalt phosphide /graphitic carbon polyhedral hybrid	Glassy carbon electrode	1 M KOH	345	56	*J. Mater. Chem. A*, 2016, **4**, 13742-13745
Ni-modified cobalt phosphide nanoparticles	Glassy carbon electrode	1 M KOH	360	82	*J. Mater. Chem. A*, 2016, **4**, 7549-7554